
Tomographic Myocardial Perfusion Imaging with Technetium-99m-Teboroxime at Rest and After Dipyridamole

Quan-Sheng Li, Gregoire Solot, Terry L. Frank, Henry N. Wagner, Jr., and Lewis C. Becker

Department of Medicine, Division of Cardiology, and Department of Radiology, Division of Nuclear Medicine, The Johns Hopkins Medical Institutions, Baltimore, Maryland

This study was done to determine whether the rapidly clearing myocardial perfusion agent ^{99m}Tc -teboroxime (SQ 30217, Cardiotec[®]) could be combined with tomographic imaging to accurately quantify regional myocardial blood flow distribution in anesthetized dogs. Following stenosis of the anterior descending (LAD, $n = 10$) or circumflex (LCX, $n = 5$) coronary arteries, teboroxime was administered simultaneously with radioactive microspheres, at rest and following infusion of dipyridamole ($0.15 \text{ mg/kg/min} \times 4 \text{ min}$). Tomographic imaging began 1 min after each teboroxime injection and continued for 12 min. For LAD stenosis, when the dipyridamole study was performed first, teboroxime activity in the center of the ischemic region was closely correlated with tissue microsphere content. However, the severity of the dipyridamole-induced flow deficit was underestimated by teboroxime when the rest study was performed first. Our results show that despite rapid myocardial clearance, tomographic imaging of ^{99m}Tc -teboroxime provides reasonably accurate quantitation of dipyridamole-induced anterior wall perfusion defects, but that the flow deficit is underestimated when a rest study is performed first or when the defect is located in the inferior wall.

J Nucl Med 1991; 32:1968-1976

Technetium-99m-teboroxime ((bis[1,2-cyclohexanedione-dioximato (1-)-O]-[1,2-cyclohexanedione dioximato (2-)-O] methyl-borato (2-)-N,N',N'',N''',N''''-chlorotechnetium), also known as SQ 30217 or Cardiotec[®], is a neutral lipophilic technetium complex that holds promise as a myocardial perfusion agent. Preclinical testing of ^{99m}Tc -teboroxime in dogs has demonstrated high quality myocardial images (1,2) and clinical trials have yielded results comparable to ^{201}Tl in patients with coronary artery disease (1,3-7). However, ^{99m}Tc -teboroxime has the novel property of very rapid myocardial clearance. About half of the initial myocardial activity is gone within 10-15 min

after intravenous injection, necessitating the acquisition of images within a very short time frame (2,6,8,9). After 15 min, myocardial activity is generally too low and hepatic activity too high to permit adequate myocardial imaging.

Because of rapid tracer clearance, serial stress/rest myocardial imaging should be possible without the confounding effects of residual myocardial activity. However, rapid clearance also confers significant constraints on the imaging protocol. So far, most clinical studies have utilized planar imaging, apparently in the belief that tomographic imaging is not feasible during a period of rapidly falling myocardial activity. Tomographic reconstruction algorithms assume a constant radioactive tracer distribution within the field of interest (10). To the extent that tracer distribution changes during sequential projection images, artifacts or distortions may be created (11,12).

This study was designed to determine the feasibility and quantitative accuracy of tomographic myocardial imaging with ^{99m}Tc -teboroxime, utilizing a canine model of coronary artery stenosis in which regional myocardial perfusion could be measured with radioactive microspheres. Serial ^{99m}Tc -teboroxime imaging was performed before and after administration of intravenous dipyridamole, and the quantitative distribution of ^{99m}Tc -teboroxime in the reconstructed tomograms was compared to the distribution of myocardial blood flow to determine whether significant errors were introduced by the tomographic imaging approach.

MATERIALS AND METHODS

Sterile pyrogen-free ^{99m}Tc -teboroxime was prepared from a kit provided by Squibb Diagnostics (Princeton, NJ). Twenty-five millicuries of [^{99m}Tc]pertechnetate in 0.1-3.0 ml was added to the kit, and the vial was placed in a boiling water bath for 15 min. After the vial had cooled, radiochemical purity was checked by chromatographic analysis. The radiochemical purity was greater than 95% in all cases.

Fifteen mongrel dogs of either sex weighing 40-60 pounds were anesthetized with sodium pentobarbital, intubated and ventilated with a Harvard respirator. Cannulae were placed in the femoral artery for blood sampling, and in the femoral vein for injection of tracer. A left thoracotomy was performed in the fifth

Received Feb. 12, 1990; revision accepted Jun. 4, 1991.
For reprints contact: Lewis C. Becker, MD, The Johns Hopkins Hospital, 600 N Wolfe St., Halsted 500, Baltimore, MD 21205.

intercostal space. In the first series of experiments, a proximal segment of the left anterior descending coronary artery (LAD) (Group 1, $n = 5$) or the left circumflex coronary artery (LCX) (Group 2, $n = 5$) was isolated and an electromagnetic flow probe placed around the artery (BL-613, Biotronix, Kensington, MD). A plastic clamp with a screw adjustment was placed around the coronary artery proximal to the flow probe and a black silk snare was placed just distal to the flow probe to provide transient cessation of flow. The baseline reactive hyperemic response following a 10-sec flow occlusion was then recorded, and the screw occluder was tightened to eliminate peak reactive hyperemia without reducing resting flow, after which the flow probe was removed and the dog was transferred to the imaging suite.

With the dog positioned on its back under a tomographic gamma camera, dipyridamole was infused intravenously by a Harvard pump (0.15 mg/kg/min for 4 min in 20 ml physiological saline). Technetium-99m-teboroxime, 4 mCi, was injected intravenously 4 min after the end of the dipyridamole infusion. At the same time, 2×10^6 ^{125}I -microspheres (3M Products) with a diameter of 8–10 μm were injected into the left atrium. Arterial blood samples were withdrawn by a Harvard pump at a constant rate of 2.16 ml/min, starting just before injection of microspheres and continuing for 2 min afterward for determination of regional myocardial blood flow. Tomographic images were begun 1 min after injection of the $^{99\text{m}}\text{Tc}$ -teboroxime and took approximately 12 min to complete. A second dose of $^{99\text{m}}\text{Tc}$ -teboroxime, 6 mCi intravenous, and 2×10^6 ^{153}Gd microspheres (DuPont Co.) were given simultaneously 30 min after the end of the first imaging acquisition. A second set of tomographic images was obtained over 12 min beginning 1 min after the second $^{99\text{m}}\text{Tc}$ -teboroxime injection.

In a separate series of animals, the rest study was performed before the dipyridamole study (Group 3, $n = 5$). The proximal LAD was stenosed as described above, after which $^{99\text{m}}\text{Tc}$ -teboroxime, 4 mCi intravenous, was injected at rest along with 2×10^6 ^{125}I radioactive microspheres. Tomographic imaging was begun 1 min after injection of $^{99\text{m}}\text{Tc}$ -teboroxime and continued for approximately 12 min. Thirty minutes after completion of imaging, 0.15 mg/kg/min dipyridamole was infused intravenously for 4 min, and 4 min after completion of the infusion, 6 mCi of $^{99\text{m}}\text{Tc}$ -teboroxime was injected, along with 2×10^6 ^{153}Gd radioactive microspheres, and tomographic imaging was repeated. In four of the dogs, dipyridamole was infused again in the same dose 45 min later, 8 mCi $^{99\text{m}}\text{Tc}$ -teboroxime and 2×10^6 ^{103}Ru radioactive microspheres (DuPont Co.) were injected, and tomographic imaging was performed with a more rapid 5 min acquisition protocol beginning one min after injection.

Tomographic imaging was performed with a Technicare Omega 500 rotating large field of view camera, which acquired 30 images (20 sec/image for most studies) through 180° from the right lateral to the left lateral position (total imaging time 12 min). For 5 min tomographic acquisitions, the protocol was the same except that projection images were acquired for 8 sec. A high-resolution parallel-hole collimator was used, with a 20% energy window centered on the 140 keV gamma-ray peak. Raw images were obtained in 128 \times 128 byte mode with a 1.4 camera magnification and a 22-cm radius of rotation. Filtered backprojection, using a Hanning 0.65 filter, was performed using a nuclear medicine computer (Technicare Model 560). The data were then reoriented to display 6–7 serial 1.0-cm thick short-axis slices from apex to base of the left ventricle.

Four short-axis slices from each heart, representing most of the left ventricle except for the apex and base, were displayed in 64 \times 64 byte mode and subjected to a semi-automated analysis of regional $^{99\text{m}}\text{Tc}$ -teboroxime content. The radial distribution of imaged $^{99\text{m}}\text{Tc}$ -teboroxime activity was quantitated using our modification of the "CIRMAX" circumferential profile program provided by Technicare. As in the standard program, the operator generates a region of interest by positioning a circle just outside of the outer perimeter of the myocardial slice. For each angular interval, the program finds the pixels which lie along the radial line at the desired angle, and determines the maximum count. The CIRMAX curve begins at 3 o'clock and proceeds counter-clockwise. Unlike the standard program, however, the curve is normalized by the value located exactly 180° opposite the nadir of the curve, rather than by the highest value in order to allow better matching with the tissue microsphere data (13).

After euthanization with KCl, the heart was removed, the right ventricle excised, and the left ventricle was sectioned transversely from apex to base into 6–7–1.0-cm thick slices, corresponding to the number and thickness of the short-axis tomographic images. Four mid-left ventricular rings were selected, and each was divided radially into 12 samples that were weighed and counted in a scintillation counter (Packard Auto Gamma Scintillation Spectrometer Model 5986) along with the reference blood samples. Pulse-height analysis was used to differentiate activity from the three or four radionuclides present ($^{99\text{m}}\text{Tc}$, 124–170 keV; ^{153}Gd , 36–54 keV; ^{125}I , 10–34 keV; ^{103}Ru , 446–550 keV). The $^{99\text{m}}\text{Tc}$ -teboroxime activity was counted immediately, and microsphere activities were measured two days later.

Regional myocardial blood flow (RMBF) was calculated using the formula: $\text{RMBF} = R (\text{Cm}/\text{Cr}) (\text{ml}/\text{min}/\text{g})$, where R = reference blood flow pump withdrawal rate, Cm = counts per gram in the myocardial samples, and Cr = counts in the reference blood sample (14). For each left ventricular slice, the RMBF of each sample was normalized by the RMBF of the sample located 180 degrees away from the center of the ischemic zone, and expressed as a ratio.

Kinetic Studies

To determine the clearance rate of $^{99\text{m}}\text{Tc}$ -teboroxime from myocardium both at rest and during dipyridamole infusion, four normal dogs were anesthetized and the camera detector was placed in a 15° left anterior oblique (LAO) position over the heart. Technetium-99m-teboroxime, 1.5 mCi, was injected intravenously, and immediately afterwards, a set of dynamic planar images was begun and continued for 30 min (30 sec/view, 64 \times 64 byte mode). Dipyridamole, 0.15 mg/kg/min, was then infused intravenously for 4 min, 30 min after completion of the first set of images. A second dose of $^{99\text{m}}\text{Tc}$ -teboroxime (2 mCi) was injected intravenously 4 min after completion of the dipyridamole infusion, and a second set of dynamic images was immediately begun. Regions of interest (ROI) for myocardium (away from the liver) and liver (away from the gallbladder) were drawn, and the densities (counts/pixel) of these ROI were averaged at each time point for the four animals. The serial count density data were fit to a two-compartment model using a computerized nonlinear curve fitting program (PC NONLIN). Data were fit to the equation:

$$C = Ae^{-\alpha t} + Be^{-\beta t},$$

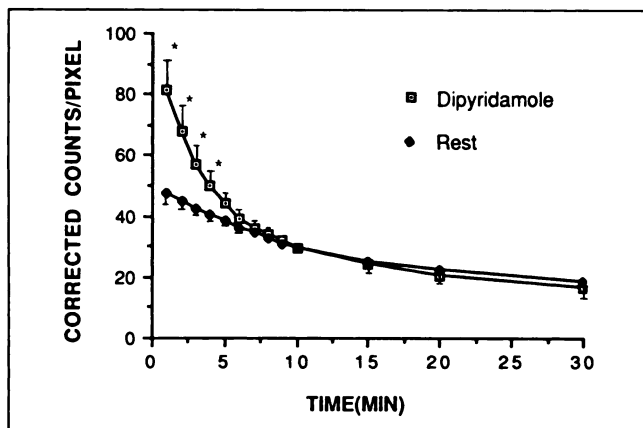


FIGURE 1. Mean myocardial time-activity curves following intravenous ^{99m}Tc -teboroxime injection at rest, followed by repeat injection after dipyridamole. Values are corrected for decay and expressed per mCi injected dose. Note greater initial uptake and more rapid early clearance after dipyridamole, with equalization of curves by 7 min. * $p < 0.05$ versus corresponding Rest value.

where C = count density, t = time following injection, α = first-phase rate constant, β = second-phase rate constant, and A and B are constants.

Phantom Studies

To examine the effect of time-related count losses during tomographic acquisition, studies were performed utilizing a plastic SPECT phantom (Data Spectrum Corp., Chapel Hill, NC) with a cardiac insert simulating the left ventricle. The chamber representing the "myocardium" (width = 0.8 cm) was filled with water containing [^{99m}Tc]pertechnetate except for two full thickness solid plastic sectors (45° arc) representing "perfusion defects" in the "inferior wall" and "lateral wall." The cardiac insert was mounted inside the SPECT phantom cylinder (21.6 cm diameter) obliquely from the long axis to simulate normal heart position in the thorax. The phantom was filled with water without ^{99m}Tc . Tomographic acquisition (30 projection angles over 180°) and slice reconstruction was performed as in the in vivo dog studies. The projection images contained 2700 to 6900 counts, while the reconstructed short axis tomogram contained about 9000 counts.

The phantom studies were used to address the issue of whether the closeness of the defect to the camera influenced apparent defect severity in the face of rapidly falling myocardial activity. The geometry of the phantom was such that the "lateral wall" defect was closest to the camera head at the end of the acquisition (image 30) and furthest from the camera head at the beginning of acquisition (image 1), while the "inferior defect" was near the

center of rotation. First, to simulate time-related count losses, the serial projection images were divided by a constant to reduce counts by 50% or 99% from image 1 to 30 (count reduction of 1.7% or 3.3% per projection image). This simulated the situation where a perfusion defect might be further from the camera when the myocardial counts were highest and closer to the camera when counts are lowest. Then the counts were reduced by 50% or 99% in the reverse direction (image 30 to image 1) to simulate the opposite situation, where the defect might be closer to the camera when counts are highest and further from the camera when counts are lowest. Image sets with simulated count losses were reconstructed with the same parameters as the original image set, subjected to circumferential profile analysis of selected short axis slices, and compared quantitatively to the original image set.

Statistical Analysis

Results are expressed as the mean \pm s.d. The paired t-test was used to determine the significance of mean differences in the quantitative curves between ^{99m}Tc -teboroxime tomograms and microsphere tissue-counting and between dipyridamole and rest studies. A p value of 0.05 or less was considered significant.

RESULTS

Kinetic studies demonstrated very rapid clearance of ^{99m}Tc -teboroxime from the myocardium. Serial planar imaging showed high quality myocardial images for the first several minutes, but by 15 min image quality was markedly impaired due to the combination of falling myocardial activity and increasing hepatobiliary uptake. The mean heart/liver activity ratio decreased from 1.35 at 1 min postinjection to 0.53 at 15 min. Myocardial activity curves demonstrated that initial uptake of ^{99m}Tc -teboroxime was greater following dipyridamole than at rest, but by 7 min the curves became nearly superimposable (Fig. 1). The curves at rest and following dipyridamole both appeared to be biexponential. Quantitative analysis of the fast and slow components is presented in Table 1.

Despite rapid myocardial clearance, tomographic images of the myocardium acquired over the first 12 min were of good quality. Figure 2 shows representative short axis slices from a dog in Group 1 with anterior descending coronary artery stenosis, in which the dipyridamole study was performed before the "rest" study. The dipyridamole image shows a marked anterior perfusion defect, confirmed by the quantitative ^{99m}Tc -teboroxime and microsphere profile curves. The "rest" image, obtained about 45

TABLE 1
Biexponential Analysis of Myocardial Clearance Curves

	Fast phase		Slow phase		Time to 50% count loss (min)
	Compartment size (%)	$T_{1/2}$ (min)	Compartment size (%)	$T_{1/2}$ (min)	
Rest (n = 4)	37.5 ± 12.5	4.6 ± 1.1	62.6 ± 12.5	47.6 ± 8.4	19.5
Dipyridamole (n = 4)	57.9 ± 4.7	2.3 ± 0.6	42.2 ± 4.7	58.8 ± 27.9	5.4

Values represent mean \pm s.d.

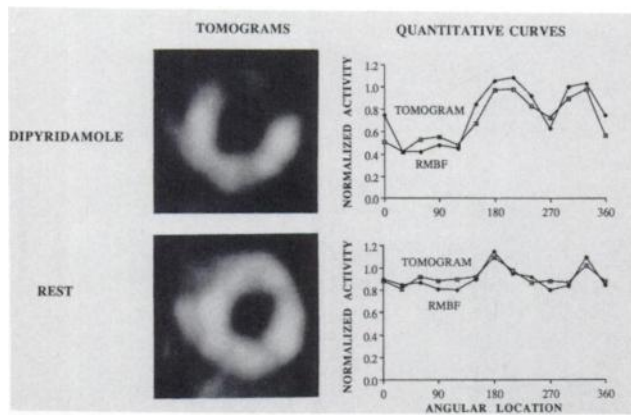


FIGURE 2. Panels represent short-axis tomographic ^{99m}Tc -teboroxime images along with corresponding quantitative circumferential profile curves (SQ (TOMO)) and matched tissue microsphere activity curves (RMBF) for serial studies after dipyridamole in a dog from Group 1 with anterior descending coronary artery stenosis. Note marked perfusion defect 4 min after dipyridamole with good agreement between the ^{99m}Tc -teboroxime and microsphere activity curves. The defect is much less marked after repeat injection of ^{99m}Tc -teboroxime 45 min later ("rest" study).

min later, shows a considerable reduction in defect intensity, corresponding to a less severe reduction in normalized microsphere blood flow. Early after dipyridamole, for the five dogs with LAD stenosis in Group 1 (20 left ventricular rings) the mean nadir of the normalized activity curve was 0.53 ± 0.24 for ^{99m}Tc -teboroxime and 0.49 ± 0.32 for microspheres (Table 2). At "rest," the mean nadir rose to 0.75 ± 0.13 for ^{99m}Tc -teboroxime and 0.85 ± 0.27 for microspheres ($p < 0.0001$ versus dipyridamole for both, $p = \text{n.s.}$ for ^{99m}Tc -teboroxime versus microspheres).

Figure 3 shows representative short-axis slices from a dog with circumflex coronary artery stenosis from Group 2. The dipyridamole image shows a moderate inferior perfusion defect confirmed by the quantitative ^{99m}Tc -teboroxime and microsphere curves. The "rest" images obtained 45 min later shows partial resolution of the defect and less reduction of activity in the inferior wall on quantitative analysis. Note that in the dipyridamole study,

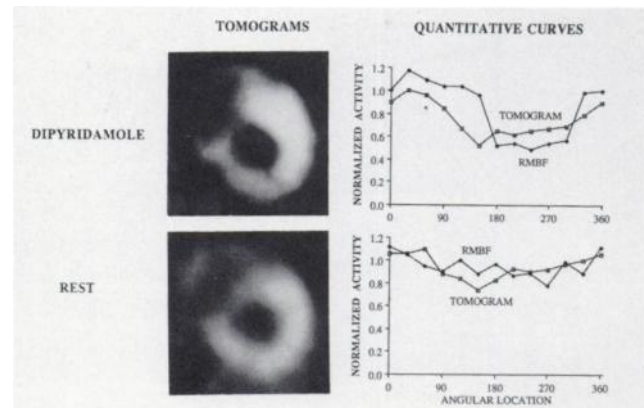


FIGURE 3. Images and curves in a dog with circumflex coronary artery stenosis (Group 2). Note marked perfusion defect 4 min after dipyridamole, much improved after repeat ^{99m}Tc -teboroxime injection 45 min later ("rest" study). Also note underestimation of flow deficit in the inferior wall by ^{99m}Tc -teboroxime (TOMOGRAM) compared to microspheres (RMBF). This probably represents scatter from hepatobiliary activity.

^{99m}Tc -teboroxime underestimates the severity of ischemia in the inferior wall. After dipyridamole, for the five dogs with circumflex stenosis in Group 2 (20 LV slices) the mean nadir of the normalized activity curve was 0.53 ± 0.23 for ^{99m}Tc -teboroxime versus 0.30 ± 0.30 for microspheres ($p, 0.0001$). At "rest," the nadir was significantly higher for both ^{99m}Tc -teboroxime and microspheres (0.81 ± 0.29 versus 0.55 ± 0.38 , respectively; $p < 0.0001$ versus dipyridamole for both), but ^{99m}Tc -teboroxime activity still overestimated microsphere content ($p = 0.0001$).

Figure 4 shows representative short-axis slices from a dog with an anterior descending coronary artery stenosis from Group 3. The rest image shows relatively homogeneous tracer uptake without a significant perfusion defect, confirmed by the quantitative ^{99m}Tc -teboroxime and microsphere curves. The dipyridamole image obtained about 45 min later shows a severe anterior perfusion defect. However, in contrast to the dog with LAD stenosis in Group 1 (Fig. 2), ^{99m}Tc -teboroxime underestimated the

TABLE 2
Comparison of Teboroxime and Microsphere Activity Curves

Group	Artery stenosed	First study	Dipyridamole				Rest			
			Teboroxime (TOMO)		Microspheres		Teboroxime (TOMO)		Microspheres	
			Nadir	Width	Nadir	Width	Nadir	Width	Nadir	Width
1	LAD	DIPYR	$0.53^{\dagger} \pm 0.24$	$102^{\dagger} \pm 79$	$0.49^{\dagger} \pm 0.32$	$107^{\dagger} \pm 83$	0.75 ± 0.13	40 ± 55	0.85 ± 0.27	20 ± 43
2	LCX	DIPYR	$0.53^{* \dagger} \pm 0.23$	$104^{\dagger} \pm 72$	$0.30^{\dagger} \pm 0.30$	$135^{\dagger} \pm 54$	$0.81^{*} \pm 0.29$	$50^{*} \pm 72$	0.55 ± 0.38	81 ± 77
3	LAD	REST	$0.49^{*} \pm 0.23$	$152^{\dagger} \pm 80$	$0.24^{\dagger} \pm 0.27$	$149^{\dagger} \pm 74$	$0.72^{*} \pm 0.08$	$62^{*} \pm 66$	0.65 ± 0.12	57 ± 45

Data from four left ventricular rings from each of the five dogs in each group. Values are mean \pm s.d. Nadir represents lowest value on normalized activity curve in ischemic region. Width represents the length of the activity curve (expressed in degrees) falling below a threshold value of 0.75.

* $p < 0.05$ versus corresponding microsphere value.

$^{\dagger} p < 0.05$ versus corresponding rest value.

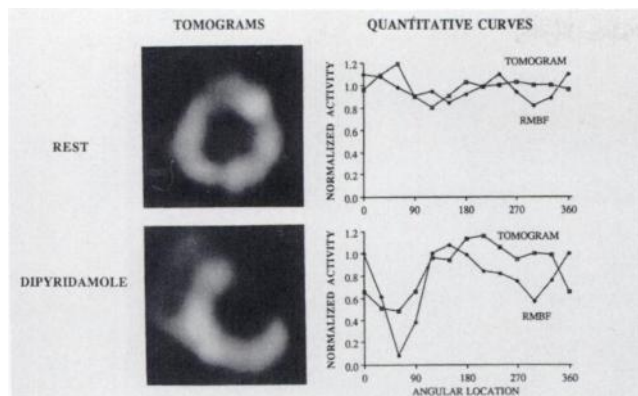


FIGURE 4. Images and curves from a dog with anterior descending coronary artery stenosis in Group 3. Note relatively homogenous perfusion at rest, followed by severe perfusion defect after dipyridamole. However, in contrast to Group 1 (Fig. 3), ^{99m}Tc -teboroxime underestimates the severity of flow deficit when the rest study is performed first.

severity of the flow deficit in the anterior wall compared to microspheres when the rest study preceded the dipyridamole study.

Figure 5 compares the perfusion defect severity measured by ^{99m}Tc -teboroxime tomography and microspheres for each left ventricular slice from the dogs in Groups 1, 2 and 3. In Group 1 (LAD stenosis, dipyridamole before "rest"), there was good agreement between ^{99m}Tc -teboroxime and microsphere estimates of ischemia (Fig. 5A). Dipyridamole points were shifted leftward relative to the "rest" points, indicative of the dipyridamole-induced flow deficit (Table 2), but remained reasonably close to the line of identity. "Rest" defects were seen in three slices from two dogs following the dipyridamole study ^{99m}Tc -teboroxime ratio < 0.6 but in two, microspheres also demonstrating persistent ischemia.

In Group 2 (LCX stenosis, dipyridamole before "rest"), ^{99m}Tc -teboroxime systematically underestimated the severity of ischemia by microspheres (Fig. 5B, Table 2). This finding was most likely related to scatter of hepatic activity,

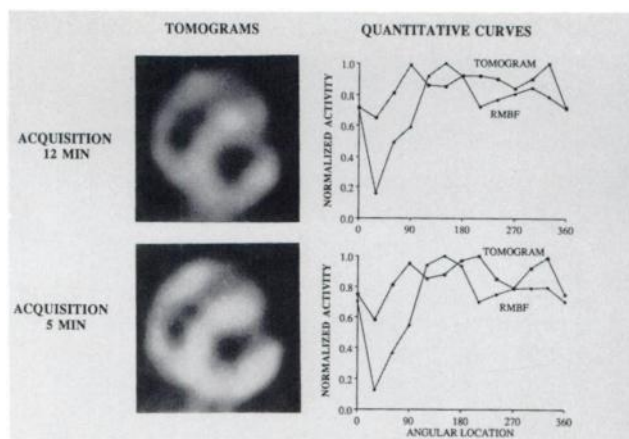


FIGURE 6. Comparison of 12 min and 5 min acquisition images of the same LV slice in serial dipyridamole studies in a dog from Group 3. Note that image quality and quantitative curves are comparable for 5 min acquisition protocol. Number of counts are 24,750/mCi for 12 min and 14,725/mCi for 5 min reconstructed image.

although there was good visual separation in all cases between the liver and the inferior left ventricular wall. Persistent defects were again seen in six of the "rest" slices obtained 45 min after the dipyridamole study and may have been related to either a tight coronary stenosis or persistent dipyridamole effect, since ischemia was confirmed by microspheres in each case.

In Group 3 (LAD stenosis, rest before dipyridamole) the rest slices were generally free of defects, although one slice demonstrated a mild ^{99m}Tc -teboroxime defect (ratio < 0.6) (Fig. 5C, Table 2). Three slices were ischemic by microspheres but had no significant ^{99m}Tc -teboroxime defect. In contrast to Group 1, however, ^{99m}Tc -teboroxime generally underestimated the severity of ischemia following dipyridamole. The most likely explanation was contamination of the dipyridamole images by residual activity from the initial rest study.

Based on the rapidity of ^{99m}Tc -teboroxime clearance following dipyridamole (Table 1), we examined the feasi-

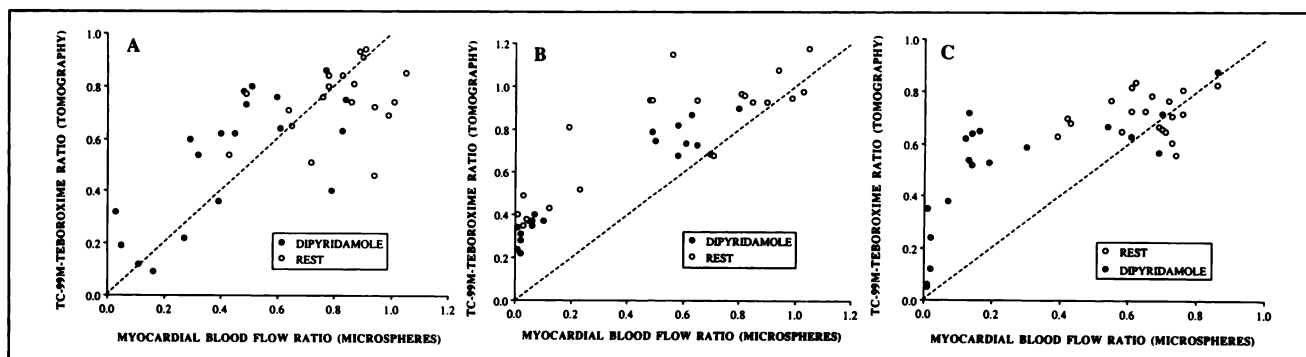


FIGURE 5. Comparison of defect severity by ^{99m}Tc -teboroxime tomography and tissue counting of microspheres. Each point represents matched scintigraphic and microsphere data from the middle of the perfusion defect in individual left ventricular slices (four per dog). Data are shown for both rest and dipyridamole studies. The dashed line is the line of identity. (A) Group 1 (LAD stenosis, dipyridamole study first). (B) Group 2 (LCX stenosis, dipyridamole study first). (C) Group 3 (LAD stenosis, rest study first).

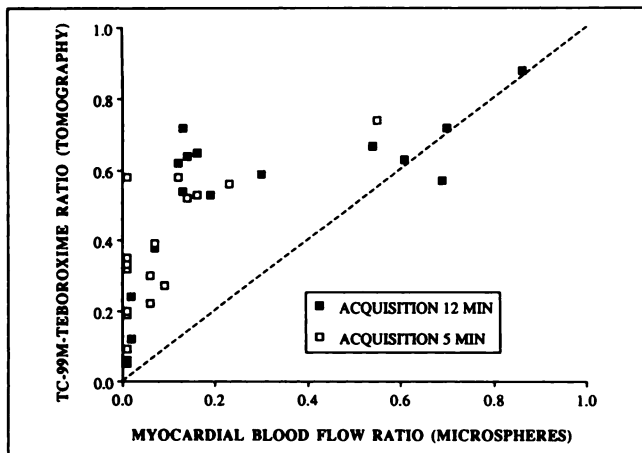


FIGURE 7. Comparison of defect severity by ^{99m}Tc -teboroxime tomography and tissue counting of microspheres for each LV slice from four dogs in Group 3 (four slices per dog). Data are shown for both 12-min and 5-min acquisition studies after dipyridamole. The 5-min studies tended to have more severe ischemia by microspheres and teboroxime, but both acquisitions demonstrated similar underestimation of flow deficit by teboroxime.

bility of 5-min tomographic acquisitions. Visually, the 5-min images were of good quality. Figure 6 compares a mid-left ventricular slice obtained following dipyridamole from a dog with an LAD stenosis (Group 3), reconstructed from separate 12-min and 5-min tomographic acquisitions. Technetium-99m-teboroxime underestimated the severity of ischemia in both studies to a similar extent. Figure 7 shows that the underestimation of dipyridamole-induced flow deficits by ^{99m}Tc -teboroxime occurred in both the 12-min and 5-min acquisition studies in each dog. Slices from the 5-min acquisition study tended to have more severe ischemia by microspheres (0.10 ± 0.14 versus 0.24 ± 0.27 , $p < 0.05$) and more severe ^{99m}Tc -Teboroxime defects (0.39 ± 0.18 versus 0.49 ± 0.24 , $p = \text{n.s.}$).

Results from the phantom study examining the effect

TABLE 3
Phantom Study: Comparison of Nadirs of Quantitative Tomographic Curves from Raw Data and Data with Simulated Count Losses

Defect location	Raw data (no count loss)	Simulated activity loss between first and last projection image	
		50%	99%
Inferior	0.28	0.29	0.28
Lateral*	0.35	0.38	0.46
Lateral†	0.35	0.30	0.22

* Defect closest to camera in last (lowest count) projection image.

† Defect closest to camera in first (highest count) projection image.

of defect location are shown in Table 3. Defect "severity" was unchanged in the "inferior wall" when the projection data were altered to mimic 50% or 99% count losses over the 12 min/180°/30 view acquisition protocol. However, when the defect was positioned in the "lateral wall," farther from the axis of rotation of the camera, the introduction of time-related count losses produced errors in apparent defect severity. The direction of the error depended on whether the defect was close to the camera at the beginning or at the end of the acquisition (i.e., when counts were at a maximum or a minimum, respectively). When the defect was nearest the camera at the *start* of acquisition, there was a 14% *overestimation* of defect severity with a simulated 50% count loss and a 37% overestimation with a 99% count loss. In contrast, when the defect was closest to the camera at the *end* of acquisition, the severity of the defect was *underestimated* by 9% and 31% at count losses of 50% and 99%, respectively.

DISCUSSION

The principal findings of this study are that despite rapid myocardial clearance, early tomographic imaging of ^{99m}Tc -teboroxime is feasible and can yield reasonably accurate quantitative information about the severity of ischemia induced by dipyridamole in the anterior wall of the left ventricle. Unfortunately, ischemia is underestimated in the inferior wall, probably due to photon scatter from the liver, and in the anterior wall when a rest study is performed first, probably due to residual activity in the myocardium. In addition, phantom studies demonstrate that over or underestimation of defect severity can occur when the ischemic region is located off the axis of rotation, depending on whether the ischemia is close to the camera at the beginning or the end of acquisition.

Technetium-99m-teboroxime represents a novel myocardial perfusion agent which, unlike the cationic agents ^{201}Tl and ^{99m}Tc -sestamibi (Cardiolite®), was designed to be electrically neutral in order to enhance its lipophilicity and passive membrane diffusion properties (2). Chemically the molecule is a bidentate chelate, in which the technetium is bound by 3 cyclohexane dione dioxime groups, which are themselves bound tightly together by a methylboron cap (15). This configuration has resulted in a molecule with very efficient myocardial uptake. Indicator dilution studies in the isolated blood perfused rabbit heart demonstrated higher myocardial extraction and capillary permeability-surface area product for ^{99m}Tc -teboroxime than for ^{201}Tl (16). In intact dogs, mean first pass retention fraction after intracoronary injection of ^{99m}Tc -teboroxime did not change as flow was increased four-fold with dipyridamole, suggesting that ^{99m}Tc -teboroxime uptake is not diffusion limited (8). Although cellular uptake of ^{99m}Tc -teboroxime is believed to occur passively, the mechanisms involved in retention and the importance of metabolic processes have not been completely defined. Using isolated monolayers of contracting chick heart cells, Kronauge et

al. (17) showed that the membrane transport inhibitors amiloride, bumetanide, verapamil and ouabain had no effect on ^{99m}Tc -teboroxime uptake, while certain metabolic inhibitors reduced uptake by up to 70%.

Despite high initial uptake, ^{99m}Tc -teboroxime is lost rapidly from the myocardium. Our own data confirm previous reports in anesthetized dogs and rats that myocardial clearance of ^{99m}Tc -teboroxime is biexponential, with a half-time of 2–4 min for the more rapidly clearing compartment and 20–98 min for the slower clearing one (2,8,9,18). The fast clearing component represents about 2/3 of retained activity (2,8,9). As in our study, the half-time of the fast component has been shown to decrease significantly following elevation of coronary blood flow with dipyridamole (8,9). Seldin et al. (3) reported somewhat slower clearance rates for ^{99m}Tc -teboroxime in normal human volunteers, but the method used for curve analysis was different from that used in the animal studies. Johnson and Seldin (6) reported that unpublished Phase I human data from Duke University demonstrated biexponential myocardial clearance with effective half-lives of 5.2 min and 3.8 hr of the two components (representing 66% and 33% of the myocardial activity, respectively). Seldin et al. (3) found that myocardial clearance was faster following exercise- than rest-injected studies.

An advantage of rapid myocardial clearance is that serial rest/exercise perfusion studies should be possible. However, our results appear to indicate that persistent activity from a first ^{99m}Tc -teboroxime study can alter the accuracy of defect quantitation in a second study performed about 50 min later.

The underestimation of ischemia following dipyridamole in Group 3 appeared to result from the earlier rest study, since it was not seen in Group 1, in which the dipyridamole study was performed first. In Group 1, persistent defects were sometimes noted on the “rest” study. This may, in part, have been due to “contamination” of the second set of images by the first, but continuing vasodilatory effects of dipyridamole were probably also responsible since microsphere flow ratios were still reduced in some left ventricular slices. Several clinical studies have demonstrated that imaging can be repeated in 1–2 hr without concern about background activity (3–6). Residual myocardial activity is usually not apparent with planar imaging (4), but can be demonstrated with tomographic imaging at 1 hr (6). Seldin et al. (3) reported persistent perfusion defects in a rest study performed after an exercise study in 10/20 patients with coronary disease, possibly related to residual myocardial activity from the exercise study (6). A similar phenomenon has been described with ^{99m}Tc -sestamibi when an exercise study is performed before a rest study in a “same-day” imaging protocol (19). However, in 8 of the 10 patients in Seldin’s study, the defect occurred in a vascular territory distal to a stenosis of $\geq 90\%$, suggesting that silent ischemia could have been present at rest.

Defect quantification in an exercise study following a rest study could in theory be improved by simply waiting longer for clearance of residual activity from the rest study. However, this approach is not very practical, since the half-time of the slowly clearing compartment is more than 3 hr in man (6). In addition, this approach nullifies what should be the unique advantage of teboroxime: the ability to perform rapid serial perfusion studies based on its rapid initial clearance. Another possibility might be to obtain a “background” image before the second study, although spatial matching and subtraction of images may prove difficult in practice. Early clinical experience suggests that identification of perfusion defects with either stress-rest or rest-stress injection sequences may be equally satisfactory (4), but it remains uncertain whether the frequency of reversible ischemia will be underestimated with protocols involving exercise imaging before rest imaging (3,4).

A theoretical disadvantage of rapid myocardial clearance is that tomographic imaging could become problematic due to either inadequate myocardial activity or artifacts created by marked loss of activity between the first and subsequent projection images. In our study, counting statistics were quite acceptable despite rapid tracer clearance. Extrapolating to a 20-mCi dose of ^{99m}Tc -teboroxime with a 12-min acquisition time, there were about 100K counts in each reconstructed short-axis tomographic slice. However, tomographic reconstruction algorithms assume a constant radioactive tracer distribution in the object being imaged. Using computer simulations, Bok et al. found that a sufficiently rapid loss of tracer resulted in image distortion and loss of resolution (12). However, distortion was minimal if tracer concentration changed less than a factor of two during one camera rotation. In our study, ^{99m}Tc -teboroxime concentration fell by a factor of about 2.2 following dipyridamole during a 12-min acquisition. Unfortunately, Bok et al. did not evaluate the effect of tracer loss on quantitation of simulated perfusion defects.

Fleming et al. (5) have recently reported that rest and exercise tomographic imaging of ^{99m}Tc -teboroxime is feasible in man using a 10-min acquisition protocol and a single-head rotating camera. Although it is unknown whether the perfusion defects were quantitatively accurate with respect to actual ischemic severity, the results agreed very well with ^{201}Tl imaging and/or quantitative coronary arteriography. The authors elected to begin tomographic imaging as soon as possible after injection of teboroxime, even to the point of stopping exercise immediately after injection. Seldin et al. (3) have suggested that tomographic imaging should begin 10 min after exercise to avoid “cardiac creep” (20) and permit data acquisition during a period of more slowly changing myocardial activity. However, methods have been developed to correct for “cardiac creep” during the early post-exercise period (21), and by waiting for 10 min, one misses the period of highest myocardial activity. Furthermore, although ^{99m}Tc -tebo-

roxime distribution is proportional to myocardial blood flow 5 min after injection, it is unknown whether this proportionality still exists 10–25 min after injection.

Although tomography may accurately quantify anterior wall defects with ^{99m}Tc -teboroxime, its rapid clearance can alter the apparent severity of defects located off the center of rotation. Based on our phantom studies, ischemia will be overestimated for defects located close to the camera at the beginning of tomographic acquisition and underestimated for defects facing the camera at the end of acquisition. However, the error was only 10%–15% for simulated count losses of 50% between the first and last projection images. In the case of a defect, particularly a mild one, not facing the camera until the final projection images, it is possible that the defect would be missed because the tomographic reconstruction would combine low count projection data containing the defect with high count data showing normal myocardium. It should be noted that our phantom study simulated time related count losses by dividing serial projection images by a constant; true loss of activity from the heart would have had a somewhat different effect on the projection data and might have yielded different quantitative results after reconstruction.

In addition, our study did not model differential tracer washout from ischemic and normal areas. Since myocardial clearance is flow-dependent (Table 1), perfusion defects induced by exercise or dipyridamole would tend to normalize with time as the ^{99m}Tc -teboroxime is washed out more rapidly from better perfused areas of myocardium. As a result, defect severity could change during data acquisition and modify the appearance of the tomographic reconstruction. This effect would be expected to exaggerate the problem of underestimation of those defects located close to the camera at the end of acquisition. The effects of differential washout can be estimated from the clearance data of Stewart et al. ($T_{1/2}$ of normal region = 5.9 min, $T_{1/2}$ of post-stenotic region = 9.3 min) (22). For acquisition of 12 min, an initial 20% defect may be obscured, since activity in the normal region falls below activity in the post-stenotic region after about 5 min. Similarly, an initial 40% defect may be missed or significantly underestimated if the defect faces the camera only at the end of acquisition. In the presence of differential clearance, sensitivity for detection of mild defects should be enhanced by shorter acquisition times.

The problem of differential washout from ischemic and normal areas of myocardium would likely be more prominent with dipyridamole than with exercise. After dipyridamole, coronary dilatation may last 30 min or more (23), while following exercise, flow usually returns to normal within a few minutes, in concert with the fall in heart rate. Nevertheless, in the study of Hendel et al. (4), some reduction in apparent defect severity was seen in 9 of 14 patients after exercise between 0–4.5 min and 4.5–9 min after tracer injection. Whether these problems of defect location relative to camera position and differential wash-

out will represent problems of practical importance in the clinical setting remains to be determined.

Initial Phase II/III clinical studies with planar imaging of ^{99m}Tc -teboroxime have been encouraging (3,4,6,7). In a multicenter trial involving 155 patients at 8 centers, sensitivity of ^{99m}Tc -teboroxime imaging was 83% with a specificity of 92% (7). Technetium-99m-teboroxime has performed similarly to ^{201}Tl for detection of coronary artery disease and identification of disease in the anterior descending, circumflex, and right coronary arteries. In many patients, the inferoapical segment on the steep left anterior oblique view was obscured by the prominent liver uptake. Although Seldin et al. (3) reported that this did not interfere significantly with detection of disease in the right coronary artery, their results showed that sensitivity for right coronary artery disease was 60% with ^{201}Tl and only 33% with ^{99m}Tc -teboroxime (3). Fleming et al. (5) reported that tomographic imaging in 30 patients provided adequate separation of the inferior left ventricular wall and liver. The detection of angiographically significant right coronary artery disease was actually better with teboroxime than ^{201}Tl . However, our own data suggest that even with good “separation,” there will still be significant scatter from the liver, resulting in an underestimation of the severity of inferior wall defects.

ACKNOWLEDGMENTS

The authors thank Anthony DiPaula, Jon Clulow and Christine G. Holzmueller for their assistance. Dr. Lyle Siddoway provided help with the compartmental analysis of myocardial ^{99m}Tc -teboroxime clearance curves. Supported by U.S. Public Health Service Grant No. 17655-15 (SCOR in Ischemic Heart Disease) from the National Heart, Lung, and Blood Institute and a gift from Mary L. Smith of the W.W. Smith Charitable Trust, Rosemont, PA.

REFERENCES

1. Coleman RE, Maturi M, Nunn AD, Eckelman WC, Juri PN, Cobb FR. Imaging of myocardial perfusion with Tc-99m-SQ 30217: Dog and human studies [Abstract]. *J Nucl Med* 1986;27:893–894.
2. Narra RK, Nunn AD, Kuczynski BL, Feld T, Wedeking P, Eckelman WC. A neutral technetium-99m complex for myocardial imaging. *J Nucl Med* 1989;30:830–837.
3. Seldin DW, Johnson LL, Blood DK, et al. Myocardial perfusion imaging with technetium-99m-SQ 30217: comparison with thallium-201 and coronary anatomy. *J Nucl Med* 1989;30:312–319.
4. Hendel RC, McSherry B, Karimeddini M, Leppo JA. Diagnostic value of a new myocardial perfusion agent, teboroxime (SQ 30,217), utilizing a rapid planar imaging protocol: Preliminary results. *J Am Coll Cardiol* 1990;16:855–861.
5. Fleming RM, Kirkeeide RL, Taegtmeier H, Adyanthaya A, Cassidy DB, Goldstein RA. Comparison of technetium-99m-teboroxime tomography with automated quantitative coronary arteriography and thallium-201 tomographic imaging. *J Am Coll Cardiol* 1991;17:1297–1302.
6. Johnson LL, Seldin DW. Clinical experience with technetium-99m teboroxime, a neutral, lipophilic myocardial perfusion imaging agent. *Am J Cardiol* 1990;66:63E–67E.
7. Zielonka JS, Cannon P, Johnson L, et al. Multicenter trial of Tc-99m-teboroxime (CardioteC): a new myocardial perfusion agent [Abstract]. *J Nucl Med* 1990;31:827.
8. Stewart RE, Hutchins GD, Brown D, et al. Myocardial retention and

- clearance of the flow tracer Tc-99m-SQ 30217 in canine heart [Abstract]. *J Nucl Med* 1989;30:860-861.
9. Stewart RE, Schwaiger M, Hutchins GD, et al. Myocardial clearance kinetics of technetium-99m SQ30217: a marker of regional myocardial blood flow. *J Nucl Med* 1990;31:1183-1190.
 10. Brooks RA, DiChiro G. Principles of computer assisted tomography (CAT) in radiographic and radioisotopic imaging. *Phys Med Biol* 1976;21:689-732.
 11. Ip WR, Holden JE, Winkler SS: A study of the image discrepancies due to object time-dependence in transmission and emission tomography. *Phys Med Biol* 1983;28:953-962.
 12. Bok BD, Bice AN, Clausen M, Wong DF, Wagner HN Jr. Artifacts in camera based single photon emission tomography due to time activity variation. *Eur J Nucl Med* 1987;13:439-442.
 13. Li QS, Frank TL, Franceschi D, Wagner HN, Jr, Becker LC. Technetium-99m-methoxyisobutyl isonitrile (RP30) for quantification of myocardial ischemia and reperfusion in dogs. *J Nucl Med* 1988;29:1539-1548.
 14. Heymann MA, Payne BD, Hoffman JIE, Rudolph AM. Blood flow measurements with radionuclide-labeled particles. *Prog Cardiovasc Dis* 1977;20:55-79.
 15. Nunn AD, Treher EN, Feld T. Boronic acid adducts of technetium oxime complexes (BATOs). A new class of neutral complexes with myocardial imaging capabilities [Abstract]. *J Nucl Med* 1986;27:893.
 16. Leppo JA, Meerdink DJ. Comparative myocardial extraction of two technetium-labeled BATO derivatives (SQ30217, SQ30214) and thallium. *J Nucl Med* 1990;30:67-74.
 17. Kronauge JF, Piwnica-Worms D, Holman BL, et al. Mechanistic comparison of neutral and cationic myocardial perfusion agents [Abstract]. *J Nucl Med* 1989;30:757.
 18. Narra RK, Kuczynski BL, Feld T, Nunn AD, Eckelman WC. A comparison of the pharmacokinetics of a new Tc-99m-labelled myocardial imaging agent, SQ 32,014 with SQ 30,217 [Abstract]. *J Nucl Med* 1987;28:674.
 19. Taillefer R, Gagnon A, Laflamme L, Gregoire J, Leveille J, Phaneuf D-C. Same day injections of Tc-99m-methoxy isobutyl isonitrile (hexamibi) for myocardial tomographic imaging: comparison between rest-stress and stress-rest injection sequences. *Eur J Nucl Med* 1989;15:113-117.
 20. Friedman J, VanTrain K, Maddahi J, et al. "Upward creep" of the heart: a frequent source of false-positive reversible defects on Tl-201 stress-redistribution SPECT [Abstract]. *J Nucl Med* 1986;27:899.
 21. Geckle WJ, Frank TL, Links JM, Becker LC. Correction for patient and organ movement in SPECT: application to exercise thallium-201 cardiac imaging. *J Nucl Med* 1988;29:441-450.
 22. Stewart RE, Heyl B, Blumhardt R, O'Rourke R, Miller DD. Differential poststenotic myocardial SQ30,217 (Cardiotec) kinetics following adenosine and dipyridamole-induced hyperemic stress [Abstract]. *J Nucl Med* 1990;31:785.
 23. Brown BG, Josephson MA, Petersen RB, Pierce CD, et al. Intravenous dipyridamole combined with isometric handgrip for near maximal acute increase in coronary flow in patients with coronary artery disease. *Am J Cardiol* 1981;48:1077-1085.